

# Kimberlites reveal 2.5 billion year evolution of a deep, isolated mantle reservoir

Jon Woodhead<sup>1\*</sup>, Janet Hergt<sup>1</sup>, Andrea Giuliani<sup>1,2#</sup>, Roland Maas<sup>1</sup>, David  
Phillips<sup>1</sup>, D. Graham Pearson<sup>3</sup>, & Geoff Nowell<sup>4</sup>

1. School of Earth Sciences, University of Melbourne, VIC 3010, AUSTRALIA
  2. Department of Earth and Planetary Sciences, Macquarie University, Sydney, NSW  
2109, AUSTRALIA
  3. Department of Earth & Atmospheric Sciences, University of Alberta, Edmonton,  
Alberta T6G 2E3, CANADA
  4. Department of Earth Sciences, Durham University, Durham DH1 3LE, U.K.
- # present address: Institute of Geochemistry and Petrology, Department of Earth  
Sciences, ETH Zurich, Clausiusstrasse 25, 8092 Zurich, SWITZERLAND

\*Corresponding author, email: [jdwood@unimelb.edu.au](mailto:jdwood@unimelb.edu.au)

1 In the widely accepted paradigm of Earth's geochemical evolution, successive extraction  
2 of melts from the mantle over the past ~4.5 billion-years formed the continental crust  
3 and produced at least one complementary, melt-depleted reservoir (Depleted MORB  
4 Mantle – DMM), now recognised as the upper mantle source of Mid Ocean Ridge  
5 Basalts (MORB)<sup>1</sup>. However, geochemical modelling, and the occurrence of high <sup>3</sup>He/<sup>4</sup>He  
6 (primordial) signatures in some volcanic rocks, suggest that volumes of relatively  
7 undifferentiated mantle may reside in deeper, isolated regions<sup>2</sup>. Some basalts from  
8 Large Igneous Provinces (LIPs) may provide temporally-restricted glimpses of the most  
9 primitive parts of the mantle<sup>3,4</sup> but key questions over the longevity of such sources on  
10 planetary timescales, and whether any actually survive today, remain unresolved.  
11 Kimberlites - small volume, volcanic rocks that are the source of most diamonds offer  
12 rare insights into aspects of Earth's deep mantle composition. Radiogenic isotope ratios  
13 measured in kimberlites of different ages allow us to map the evolution of this domain  
14 through time. Here we show that globally-distributed kimberlites originate from a  
15 single homogeneous reservoir with an isotopic composition indicative of a uniform and  
16 pristine mantle source that evolved in isolation over at least 2.5 billion years of Earth  
17 history – the only such reservoir yet identified. Subsequently, around 200 million years  
18 ago, extensive volumes of the same source were perturbed dramatically, probably due  
19 to contamination by exogenic material. The distribution of affected kimberlites suggests  
20 that this event may be related to subduction along the margin of the Pangaea  
21 Supercontinent. These results reveal a hitherto unrecognised, long-lived, globally  
22 extensive, mantle reservoir that underwent subsequent disruption, possibly heralding a  
23 significant change to large-scale mantle mixing regimes. These processes may explain  
24 why uncontaminated primordial mantle is so difficult to identify in recent mantle-  
25 derived melts.

26  
27  
28  
29  
30  
31  
32  
33  
34  
35  
36  
37  
38  
39  
40  
41  
42  
43  
44  
45  
46  
47  
48  
49  
50

Kimberlites, a group of volatile-rich, silica-poor magmas, represent the only melts known to sample the Earth's deep mantle. Diamonds brought to the surface in some kimberlite eruptions contain inclusions of minerals that can only derive from great depth – for example, majoritic garnet and ringwoodite from the transition zone<sup>5</sup>, and Mg- and Ca-perovskite from at least the upper/lower mantle boundary and possibly up to 800 km deep<sup>6</sup>. Consequently some, if not all, kimberlites likely originate from at least this depth<sup>7</sup>. Importantly, kimberlitic magmas have been erupting on Earth for at least 2.85 billion years<sup>8</sup> and thus offer a unique window into the chemical evolution of deep mantle regions across much of Earth history. This view is unavailable from Ocean Island Basalts (OIB), which are frequently used as probes of present-day mantle compositions, owing to the relative youth of the ocean basins in which they occur, and also from LIPs which are temporally and spatially restricted. We have compiled new and existing Nd- and Hf-isotope data for kimberlites, distributed worldwide, and encompassing samples with well-determined eruption ages ranging spanning more than 2 billion years (Supplementary data). We restrict our study to samples that are predominantly petrographically and mineralogically equivalent to archetypal kimberlites and have filtered the dataset to exclude samples which may have experienced significant crustal assimilation (see Methods).

The compilation of these data reveals that, prior to ~200 Ma, the mantle source of all kimberlite bodies globally appears to have evolved along a single isotopic trajectory over more than 2 Gyr of Earth history, through the Proterozoic Eon, indicating derivation from a relatively homogeneous reservoir with a composition very close to that of the Chondritic Uniform Reservoir (CHUR) model<sup>9</sup> for Earth's Primitive Mantle – PM (Fig 1): we term this group 'primitive' kimberlites. To place this observation in perspective, the narrow isotopic variation recorded in kimberlites across the globe throughout this period is comparable to that

51 observed in the modern MORB source<sup>10</sup> (Fig 2a) and at least half of this variability (4-5  
52 epsilon units) can be accounted for through simple radiogenic ingrowth during this time (see  
53 below). That an assumed deep mantle reservoir of such homogeneity and global extent has  
54 been maintained for close to half the age of the Earth (and likely more) requires a source that  
55 is both ancient and has remained isolated from the depleted, convective upper mantle  
56 (MORB source) for the majority of this time. In fact, Fig 2b shows that the integrity of this  
57 domain is unlikely to have been maintained if substantial contamination by subducted  
58 components had occurred. The fact that kimberlite magmas originate in the deeper mantle  
59 and have tapped a homogeneous source that is compositionally distinct from DMM over a  
60 very long period of time, raises the possibility that this previously unrecognised source, of  
61 worldwide extent, may actually represent a primordial mantle composition that has remained  
62 isolated for billions of years.

63         While most kimberlites younger than 200 Ma continue to evolve along the same  
64 ‘primitive’ trajectory, samples from at least three large kimberlite fields generated after 200  
65 Ma (southern Africa, Brazil, western Canada) appear to define quite different, steeply-  
66 inclined trajectories in Nd and Hf isotope space - herein termed ‘anomalous’ kimberlites (Fig  
67 3). The origin of these steeper arrays is considered separately in a later section: however, it is  
68 important to note that, in all three areas, older (Pre-Mesozoic) samples plot along the  
69 ‘primitive’ trend whereas <200 Ma kimberlites from the same areas experienced a distinct  
70 chemical perturbation producing a sudden, dramatic decrease in source Nd and Hf isotope  
71 compositions.

72         Debates over the potential preservation of an early Earth PM, and its likely  
73 composition, continue to intrigue the geochemical community<sup>3,11,12,13</sup>. Although it has been  
74 demonstrated recently that the bulk Earth originally had a genetic evolution similar to the  
75 enstatite chondrites<sup>14</sup>, the critical question of whether *any* pristine primordial reservoirs

76 actually still exist is difficult to address. This is largely because our only evidence is provided  
77 by isolated sample suites that necessarily provide only brief ‘snapshots in time’ (e.g., the ~60  
78 Ma picrites of Baffin Island<sup>3</sup>) which may, only by coincidence, correspond to a predicted PM  
79 composition at a given point in Earth history. Kimberlite data offer a new perspective on this  
80 issue. At the most fundamental level, any surviving remnant of an early primordial reservoir  
81 must fulfil at least four criteria: it should be 1) demonstrably very long-lived, 2) relatively  
82 homogeneous, 3) compositionally distinct from the bulk of the convecting upper mantle  
83 (DMM), and 4) conform to an estimate of a primordial composition<sup>15</sup>. The mantle source of  
84 the primitive group of kimberlite magmas noted above is perhaps the only reservoir on Earth  
85 yet identified that satisfies all of these requirements. The Nd-Hf and age data reveal long-  
86 term evolution of a relatively homogeneous, deep mantle source that is isotopically distinct  
87 from DMM (Figures 1 and 2) and one that has seemingly remained isolated from significant  
88 sediment recycling for ~2 billion years of Earth history (see below). Furthermore, its isotopic  
89 evolution with time appears very close to our best estimate of a PM composition, the  
90 aforementioned CHUR model. Employing best-fit lines through the arrays in Fig.1, anchored  
91 to a CHUR isotopic composition at 4.55 Ga, we can estimate the present day isotopic  
92 composition of this reservoir ( $^{143}\text{Nd}/^{144}\text{Nd} \sim 0.512783$ ,  $^{176}\text{Hf}/^{177}\text{Hf} \sim 0.282886$ ) and the parent-  
93 daughter ratios implied by its isotopic evolution ( $^{147}\text{Sm}/^{144}\text{Nd} \sim 0.2011$  and  $^{176}\text{Lu}/^{177}\text{Hf}$   
94  $\sim 0.0347$ ). The latter appear slightly super-chondritic when compared with the reference  
95 values of 0.1960 and 0.0336, respectively, for CHUR<sup>15</sup>, but it is clear that their scatter  
96 encompasses the CHUR evolution line.

97 Other geochemical data provide corroborating evidence: for example, ratios of the  
98 less mobile trace elements, particularly Nb/Ta ( $19 \pm 5$ , 1 SD) and Nb/Th ( $11 \pm 5$ , 1 SD) in  
99 samples from the primitive kimberlite dataset are within uncertainty of PM (17.7 and 8.3  
100 respectively)<sup>16</sup> and distinct from DMM (15.5 and 18.8)<sup>17</sup> values. Other elemental ratios such

101 as La/Nb, and Ba/Nb also readily distinguish PM (~1 and ~10 respectively)<sup>16</sup> from DMM  
102 (~1.3 and ~3.8)<sup>17</sup> and crustal (~2.2 and ~52)<sup>18</sup> reservoirs. Although showing more scatter in  
103 our dataset, and despite the potential high mobility of Ba, both La/Nb and Ba/Nb ratios  
104 ( $0.8 \pm 0.4$  and  $10 \pm 10$ , 1 SD, respectively) again show similarity with PM estimates. The  
105 suggestion that the kimberlites may track a primordial source is also supported by noble gas  
106 isotope systematics in fresh kimberlitic olivine:  $^3\text{He}/^4\text{He}$  ratios up to  $27R_A$  ( $R_A$  denotes the  
107 atmospheric value =  $1.4 \times 10^{-6}$ ) in samples from Greenland (including samples used in this  
108 study) suggest derivation from a relatively undegassed mantle<sup>19</sup>, while Ne isotopes from  
109 Siberian samples indicate a deep source ‘more primitive than MORB or the Sub-Continental  
110 Lithospheric Mantle’<sup>20</sup>. We therefore contend that the kimberlite source, and in particular that  
111 sampled prior to 200 Ma, may represent a surviving remnant of early mantle uncontaminated  
112 by extensive subduction recycling. If this is the case then the composition recorded appears to  
113 require slightly super-chondritic Sm/Nd and Lu/Hf ratios, but with the scatter in the data  
114 encompassing assumed CHUR values.

115         Although the primitive kimberlite source remained very close to CHUR throughout its  
116 evolution, and some of the limited displacement can be explained by radiogenic ingrowth  
117 alone (even slightly non-chondritic parent/daughter ratios will lead to divergence from  
118 CHUR with time – see trajectory in Fig.2b), we have considered alternative scenarios capable  
119 of generating the subtle super-chondritic compositions observed. For example, it has been  
120 shown that mixtures of ancient recycled basalt and sediment, incorporated into the mantle,  
121 may explain the present-day Nd-Hf isotopic compositions of OIB and MORB<sup>21</sup>. Following a  
122 similar reasoning, we explored the effect of subducting slab-derived materials into a PM  
123 mantle source. Under these scenarios we find a best fit to the primitive kimberlite data array  
124 is achieved by continual 5% admixture of a slab component that is generated ~500 million  
125 years prior to mixing with the mantle source region (Extended Data Figure1, see Methods):

126 contributions of 0-10% slab of 0.5-1.0 Ga age can be accommodated given the scatter in the  
127 data. When using higher slab:mantle ratios and/or older slab materials, calculated mixtures  
128 develop sub-chondritic Hf-isotope values limiting involvement to relatively youthful (<~0.5  
129 Ga) slabs. In all of these models, preservation of linear arrays with time requires consistent  
130 slab ageing scenarios and similar mixing proportions to be maintained throughout time and  
131 space. Note that these experiments were conducted without any attempt to model elemental  
132 fractionation in the slab assemblage during its transit through a subduction zone since the  
133 outcomes of this process are very poorly constrained for the Lu-Hf system. It is thought,  
134 however, that subduction zone processes will raise the Sm/Nd ratio of the slab residue<sup>22</sup> and  
135 thus lead to a reduction in the proportion of slab component that could be accommodated by  
136 the primitive kimberlite data array.

137         It remains plausible, therefore, that subduction of basaltic slabs ( $\pm$ sediment) into the  
138 deeper mantle has the potential to account for our results; however a somewhat restrictive set  
139 of circumstances would be required to generate the linear arrays defined by the kimberlite  
140 data (Fig. 1). Moreover, such a scenario does not detract from our primary conclusion as a  
141 primordial source would be required as a starting point for any such mixing events. On  
142 balance, the evolution of a single deep, isolated mantle source, with slightly super-chondritic  
143 parent/daughter ratios offers the simplest explanation of the data and requires the least  
144 number of assumptions and special conditions. The model also best accounts for the observed  
145 high  $^3\text{He}/^4\text{He}$  ratios reported for some kimberlites and values of key incompatible trace  
146 element ratio values.

147         In the three ‘anomalous’ kimberlite suites erupted after 200 Ma, transition to their  
148 perturbed state appears to have been very rapid, occurring over a few tens of Ma (e.g.,  
149 primitive Jwaneng kimberlite at 235 Ma vs. anomalous Silvery Home kimberlite at 181 Ma in  
150 southern Africa), and likely represents the effects of a single event of regional extent. At this

151 time, the kimberlite source was dramatically modified by a low  $^{143}\text{Nd}/^{144}\text{Nd}$  and  $^{176}\text{Hf}/^{177}\text{Hf}$   
152 component (Fig.3). A recent study of boron isotope variations in carbonatites worldwide<sup>23</sup>  
153 also shows a major isotopic and elemental perturbation around this time towards material  
154 with an apparent subduction influence. Global plate tectonic reconstructions for the period  
155 immediately preceding the development of the anomalous kimberlites (Extended Data Figure  
156 2) indicate that the three areas showing perturbed isotopic evolution in our dataset (Mesozoic  
157 kimberlites from southern Africa, Brazil and western Canada), are all closest to a major  
158 subduction zone along the western (Panthalassan) margin of the Pangaea Supercontinent. We  
159 therefore suggest that the lowering of Nd-and Hf-isotope ratios at ~200 Ma may be  
160 subduction-related. A popular model for the breakup of Supercontinents<sup>24,25</sup> involves  
161 subducting slabs, stagnating at the mantle transition zone, then episodically avalanching into  
162 the lower mantle, producing plume-related magmatism. As the breakup of Pangea was  
163 already underway at 200 Ma, we speculate that such an avalanche may have been responsible  
164 for contaminating the post-200 Ma kimberlite reservoir in a similar manner to the events  
165 proposed for the formation of inclusions in deeply sourced kimberlitic diamonds<sup>26</sup>.  
166 Modelling reveals that the isotopic departures observed in the southern Africa and western  
167 Canada kimberlites could be generated by reactivation of ancient subducting slabs - Fig 3,  
168 Methods). However, it is important to also stress that these events only affected those  
169 kimberlite sources close to the Panthalassan margin and that unpolluted 'primitive' kimberlite  
170 sources apparently still existed at that time (e.g., Tanzania, West Greenland). One further  
171 important implication of our data is that the unique isotopic characteristics of some kimberlite  
172 magmas – their departure from the so-called Hf-Nd mantle array<sup>27</sup> – is in fact a relatively  
173 youthful feature, and one confined to a restricted group of kimberlites whose source was  
174 affected by a major geochemical perturbation ~200 million years ago.

175           If the kimberlite source is indeed representative of an early formed mantle  
176 composition, then the data presented here indicate that this mantle domain – at least the part  
177 tapped by the primitive kimberlites - remained largely isolated for much of Earth history,  
178 with dramatic events around 200 million years ago then producing irreversible contamination  
179 of this source in at least three distinct regions. In the current dataset signs of any similar  
180 disruptive events occurring prior to 200 Ma are difficult to detect due, in large part, to poor  
181 chronological constraints within suites and the sparse data for older kimberlite occurrences.  
182 Although we cannot dismiss the possibility of earlier disruptive episodes, it is conceivable  
183 that the substantive ~200 Ma event recorded in the global kimberlite (and carbonatite)  
184 datasets marks an important turning point in the evolution of Earth’s mantle - from a situation  
185 where any primordial mantle(s) remained largely physically isolated, to a regime in which  
186 subducting slabs penetrated into the lower mantle with much greater regularity - as is  
187 observed at the present day<sup>28</sup>. As such, these observations might go some way to explaining  
188 one of the most intractable problems of Earth evolution, namely the apparent paradox  
189 between present day geophysical observations of whole mantle convection and geochemical  
190 arguments based upon OIB and MORB chemistry indicating substantive isolation of key  
191 mantle reservoirs in the past.

192

### 193 **References from main text**

- 194 1. Hofmann, A.W. Chemical differentiation of the Earth: the relationship between mantle,  
195 continental crust, and oceanic crust. *Earth Planet. Sci. Lett* **90**, 297-314 (1988).
- 196 2. Hofmann, A.W. Sampling mantle heterogeneity through oceanic basalts: isotopes and trace  
197 elements. *Treatise on Geochemistry 2<sup>nd</sup> edition*. p. 67-101 (2014).
- 198 3. Jackson, M.G. et al., Evidence for the survival of the oldest terrestrial mantle reservoir.  
199 *Nature* **466**, 853- 856 (2010).

- 200 4. Jackson, M.G. & Carlson, R.W. An ancient recipe for flood basalt genesis. *Nature* **476**,  
201 316-320 (2011).
- 202 5. Pearson, D.G., et al. Hydrous mantle transition zone indicated by ringwoodite included  
203 within diamond. *Nature* **507**, 221–224 (2014).
- 204 6. Nestola, F. et al. CaSiO<sub>3</sub>-perovskite in diamond confirms the recycling of oceanic crust  
205 into the lower mantle. *Nature*, **555**, 237-241 (2018).
- 206 7. Torsvik, T.H., Burke, K., Steinberger, B., Webb, S.J., Ashwal, L.D. Diamonds sampled by  
207 plumes from the core–mantle boundary. *Nature* **466**, 352-355 (2010).
- 208 8. Henning, A., Kiviets, G., Kurszlaukis, S., Barton, E., Mayaga- Mikolo, F. Early  
209 Proterozoic metamorphosed kimberlites from Gabon. *8th International Kimberlite*  
210 *Conference Long Abstract*, 4 pp (2003).
- 211 9. DePaolo, D.J., Wasserburg, G.J., Nd isotopic variations and petrogenetic models. *Geophys.*  
212 *Res. Lett.* **3**, 249-252 (1976).
- 213 10. Salters, V.J. M., Mallick, S., Hart, S.R., Langmuir, C.E., & Stracke, A. Domains of  
214 Depleted Mantle: New Evidence from Hafnium and Neodymium Isotopes. *Geochem.*  
215 *Geophys. Geosyst.* **12** (8) doi:10.1029/2011gc003617 (2011).
- 216 11. Lyubetskaya, T. & Korenaga, J. Chemical composition of the Earth’s primitive mantle  
217 and its variance: 1. Method and Results. *Journal of Geophysical Research* **112**, B03211  
218 (2007).
- 219 12. Palme, H., & O’Neill, HStC. Cosmochemical estimates of mantle composition. *Treatise*  
220 *on Geochemistry 2<sup>nd</sup> edition*. p.1-39 (2014).
- 221 13. Trela, J. et al. The hottest lavas of the Phanerozoic and the survival of deep Archaean  
222 reservoirs. *Nature Geoscience* **10**, 451–456 (2017).
- 223 14. Bouvier, A. & Boyet, M. Primitive solar system materials and Earth share a common  
224 initial <sup>142</sup>Nd abundance. *Nature* **537**, 399-405 (2016).

- 225 15. Bouvier, A., Vervoort, J.D., & Patchett, P.J. The Lu-Hf and Sm-Nd isotopic composition  
226 of CHUR: constraints from unequilibrated chondrites and implications for the bulk  
227 composition of the terrestrial planets. *Earth Planet Sci. Lett.* **273**, 48-57 (2008).
- 228 16. McDonough, W.F. & Sun, S-s. The composition of the Earth. *Chemical Geology* **120**,  
229 223-253.
- 230 17. Workman, R.K. & Hart, S.R. Major and trace element composition of the depleted  
231 MORB mantle (DMM). *Earth Planet Sci. Lett.* **231**, 53-72.
- 232 18. Rudnick, R.L. & Gao, S. Composition of the continental crust. *Treatise on Geochemistry*  
233 (2<sup>nd</sup> edition) v.4, 1-51 (2014)
- 234 19. Tachibana, Y., I. Kaneoka, A. Gaffney, & B. Upton, Ocean-island basalt-like source of  
235 kimberlite magmas from West Greenland revealed by high <sup>3</sup>He/<sup>4</sup>He ratios, *Geology* **34**,  
236 273–276 (2006).
- 237 20. Sumino, H., Kaneoka, I., Matsufuji, K., & Sobolev, A.ZV. Deep mantle origin of  
238 kimberlite magmas revealed by neon isotopes. *Geophysical Research Letters* **33**,  
239 doi:10.1029/2006GL027144 (2006).
- 240 21. Chauvel, C., Lewin, E., Carpentier, M., Arndt, N.T. & Marini, J-C. Role of recycled  
241 oceanic basalt and sediment in generating the Hf-Nd mantle array. *Nature Geoscience*  
242 doi:10.1038/ngeo.2007.51 (2008).
- 243 22. Porter, K.A. & White, W.M. Deep mantle subduction flux. *Geochemistry Geophysics*  
244 *Geosystems* **10**, doi:10.1029/2009GC002656
- 245 23. Hulett, S.R.W., Simonetti, A., Rasbury, E.T. & Hemming, N.G. Recycling of subducted  
246 crustal components into carbonatite melts revealed by boron isotopes. *Nature Geoscience*  
247 **9**, 904-908 (2016).
- 248 24. Condie, K.C., 2004. Supercontinents and superplume events: distinguishing signals in the  
249 geologic record. *Physics of the Earth and Planetary Interiors* **146**, 319–332.

- 250 25. Maruyama, S., Santosh, M. & Zhao, D., Superplume, supercontinent, and post-  
251 perovskite: mantle dynamics and anti-plate tectonics on the core–mantle boundary.  
252 *Gondwana Research* **11**, 7–37 (2007).
- 253 26. Harte, B. & Richardson, S. Mineral inclusions in diamonds track the evolution of a  
254 Mesozoic subducted slab beneath West Gondwanaland. *Gondwana Research* **21**, 236-245  
255 (2012).
- 256 27. Nowell, G.M., et al. Hf isotope systematics of kimberlite and their megacrysts: new  
257 constraints on their source regions. *J. Petrology* **45**, 1583-1612 (2004).
- 258 28. van der Hilst, R.D., Widiyantoro, S., & Engdahl, E.R. Evidence for deep mantle  
259 circulation from global tomography. *Nature* **386**, 578–584 (1997).
- 260 29. Vervoort, J.D., Plank, T. & Prytulak, J. The Hf-Nd isotopic composition of marine  
261 sediments. *Geochim. Cosmochim. Acta* **75**, 5903-5926 (2011).

262

263 **Supplementary information** All data employed in this study, together with additional  
264 geochemical data, are provided in the Supplementary data file

265

266 **Acknowledgements** We thank DeBeers Group, Stuart Graham, Bruce Kjarsgaard, and Hugh  
267 O'Brien for access to samples. Matt Felgate and Alan Greig are thanked for technical  
268 assistance while Dan Sandiford advised on the use of GPlates. Rachel Chesler and Matt  
269 Felgate produced the Tanzania perovskite and Brazilian kimberlite data respectively. JW and  
270 AG acknowledge funding from the Australian Research Council. Catherine Chauvel, Alex  
271 Sobolev, and Richard Walker are thanked for detailed and insightful reviews and Steve  
272 Shirey for helpful suggestions.

273

274 **Author contributions** JW, RM and GN were responsible for the acquisition of new isotope  
275 data, JH and AG collated existing data, JW, JH and AG conducted the data analysis, all  
276 authors contributed to writing the paper.

277

278 **Author information** Reprints and permissions information available at  
279 [www.nature.com/reprints](http://www.nature.com/reprints). The authors declare no competing interests. Correspondence and  
280 requests for materials should be addressed to JW (jdwood@unimelb.edu.au).

281

282 **Data availability**

283 All data generated or analysed during the course of this study are archived at EarthChem  
284 (<http://dx.doi.org/10.1594/IEDA/111335>)

285

286 **Corresponding author** Correspondence to J.Woodhead (jdwood@unimelb.edu.au)

## Main figure legends

### **Fig.1. Isotopic evolution in the global kimberlite dataset.**

Plots of Nd and Hf isotopic evolution with time reveal two distinct evolutionary trajectories. All kimberlites formed prior to ~200 Ma (and some formed thereafter) appear to be derived from a single, relatively homogeneous source, termed ‘primitive kimberlites’ and denoted by coloured circles. At ~200 Ma, a major disruption is observed in three regions (grey squares) which subsequently exhibit a very different isotopic character. Also shown are evolutionary trends for Depleted MORB mantle (DMM), the Chondritic Uniform Reservoir (CHUR), and a linear regression through the primitive kimberlite data, anchored to CHUR at 4.55 Ga (red dotted line). [Link here to Source Data file.](#)

### **Fig.2. Kimberlites compared to Primitive Mantle.**

(a) Initial epsilon Nd-Hf diagram comparing the primitive (coloured circles) and anomalous (grey squares) kimberlites with CHUR. Symbols as for Fig 1. Also shown are modern MORB data<sup>10</sup> and the ‘terrestrial array’<sup>29</sup>.

(b) The primitive kimberlite array (grey circles) shown together with trajectories illustrating the isotopic evolution of DMM, pelagic and terrigenous sediment reservoirs from 4.55 Ga in 500 Ma intervals. Much of the variability in the primitive kimberlite array may be explained by radiogenic ingrowth in the source region alone (orange squares). The form of the array is difficult to reconcile with significant admixtures of subducted sedimentary material. [Link here to Source Data file.](#)

### **Fig.3. Isotopic perturbation in the anomalous kimberlites**

At ~200 Ma, a major disruption is observed in kimberlites from three regions (Brazil, Southern Africa, and West Canada): isotopic compositions initially fall well below the primitive kimberlite trend (shown in grey) and then appear to evolve very rapidly back towards the array. Trajectories are shown (blue lines) for model subducting slab assemblages (90% MORB: 10% terrigenous sediment), formed at different times in Earth history. Very old slabs are required to attain the isotopic shifts observed in the anomalous kimberlite dataset. [Link here to Source Data file.](#)

## Online Methods

**Filtering the dataset** In order to identify subtle isotopic changes with time, our primary consideration for inclusion of data in the compilation was that the kimberlites have robust chronological constraints. References to the relevant age determinations are provided in the Supplementary data; any literature analyses where ages are simply inferred are not used. We have also tried, wherever petrographic constraints allow, to limit our observations to true kimberlites and closely related rocks, largely avoiding lamproites and lamprophyres.

Kimberlite magmas are, by their very nature, susceptible to contamination during ascent and emplacement. Over the years a variety of methods have been developed in order to filter geochemical datasets to circumvent such effects. These range from simple petrographic observations through to more sophisticated geochemical approaches such as the Clement Contamination Index ( $CCI = [(SiO_2 + Al_2O_3 + Na_2O) / (MgO + 2K_2O)]^{30}$ ) and other methods utilizing geochemistry<sup>31,32</sup>. Unfortunately, none of these are universally applicable since the contaminants vary considerably from site to site. For the literature data compiled as part of this study, we generally relied on the assessments of the authors themselves as to which samples may have been influenced by contamination.

For our own samples, where major element analyses were available, we have adopted a minimalist approach excluding only data with a  $CCI > 1.5$  (excluded data are labelled in the Source Data file) as a precaution, although we note that no correlations can be observed between CCI and isotopic compositions even if these data are included. In the case of the Lac De Gras kimberlites, Kjarsgaard et al.<sup>31</sup> observe that the CCI does not provide a sensitive tracer of crustal contamination because crust and mantle addition produce opposing effects on the CCI index. They therefore adopt a more rigorous filter employing bulk Al or Yb or  $\ln Si/Al$  vs  $\ln Mg/Yb$ . To provide consistency, we have adopted the same filter for our own Lac de Gras data.

Only one kimberlite occurrence has been excluded in its entirety from the literature compilation – Triassic-Jurassic kimberlites from eastern North America<sup>33</sup>. These show age-progressive volcanism and appear to have a genetic association with the Great Meteor hotspot track: as such we do not consider them to be representative of the global kimberlite source reservoir.

**Major and trace element analyses** For major element analysis, samples were prepared as fused glass discs using a mixed lithium metaborate/tetraborate flux and analysed on a SPECTRO Xepos energy dispersive XRF spectrometer in the School of Earth Sciences at the University of Melbourne. Calibrations were constructed using a wide variety of internationally-recognised certified reference materials and analyses of secondary reference materials suggest accuracy generally better than 1 - 2% for most elements. Analytical reproducibility is generally better than 1% for most elements with the exception of P<sub>2</sub>O<sub>5</sub> (up to 2%) and Na<sub>2</sub>O (up to 4%).

For trace element analysis of samples analysed at the University of Melbourne, agate-milled powders were dissolved at high pressure in ‘Parr style’ dissolution vessels overnight at 150°C, and then refluxed with nitric acid to remove fluorides. Analytical and drift correction procedures follow Eggins et al.<sup>34</sup>, employing a natural rock standard for calibration, internal drift correction using multi-internal standards (<sup>6</sup>Li, <sup>84</sup>Sr, Rh, <sup>147</sup>Sm, Re and <sup>235</sup>U), external drift monitors and aggressive washout procedures. Differences from the Eggins et al.<sup>34</sup> protocol include: 1) Tm, In and Bi were not used as internal standards since they are measured as analytes; (2) Two digestions of the USGS standard W-2 are used for instrument calibration. Samples were analysed on an Agilent 7700x. The instrument was tuned to provide Cerium oxide levels of < 1%. 4 replicates of 100 scans per replicate were measured for each isotope. Dwell times were 10 milliseconds, except for Be, Cd, In, Sb, Ta, W, Tl, Bi,

which were 30 milliseconds. Long sample wash-out times of 6 minutes with solutions of 0.5% Triton X-100, 0.025% HF in 5% HNO<sub>3</sub> and 2% HNO<sub>3</sub> and long sample uptake times of 120 seconds were employed.

Trace element data used for age correction of kimberlite Nd and Hf isotope ratios from Durham University were determined on a Perkin Elmer Sciex Elan 6000 ICPMS instrument using techniques outlined in detail by Ottley et al.<sup>35</sup>. Seven repeat dissolutions of an in-house kimberlite standard K2WI yielded Sm/Nd and Lu/Hf reproducibility of 1.1% and 2.4%, respectively.

**Nd and Hf isotope ratios** The majority of new isotope ratio analyses presented here were obtained at the University of Melbourne, after sequential extraction of Hf and Nd<sup>36,37</sup>, following standard dissolution procedures. As an aside we note that, although zircons sometimes occur in kimberlites as megacrysts, their abundance is considerably less than even that of diamond, i.e. low ppm by volume. As a result, the chances of incorporating the typically cm-sized zircon megacrysts into our samples during powdering, and dissolution is essentially zero. Furthermore, a number of studies have now demonstrated that zircons<sup>27</sup> and indeed other members of the megacryst suite exhibit the same Hf-isotopic compositions as the kimberlites that entrain them. Hence, even in the highly unlikely event that rare fragments of zircon were entrained but not dissolved, the composition that we measured would be indistinguishable from the bulk rock-zircon mix.

Isotopic compositions were measured on a Nu Plasma multi-collector ICP-MS. Instrumental mass bias was corrected by internal normalization to  $^{146}\text{Nd}/^{144}\text{Nd} = 0.7219$  and  $^{179}\text{Hf}/^{177}\text{Hf} = 0.7325$  using the exponential law, and  $^{143}\text{Nd}/^{144}\text{Nd}$  and  $^{176}\text{Hf}/^{177}\text{Hf}$  are reported relative to La Jolla Nd = 0.511860 and JMC475 = 0.282160, respectively. External precisions (2 std dev)

are  $\pm 0.000020$  and  $\pm 0.000015$ , based on results for rock standards. Nd-Hf isotope data for BCR-2 acquired simultaneously with the kimberlite dataset average  $0.512637 \pm 13$  (2sd, n=4) and  $0.282866 \pm 16$  (2sd, n=5), consistent with reference values<sup>38</sup>. Sm/Nd and Lu/Hf ratios for age corrections were calculated from high-precision trace element data obtained by quadrupole ICP-MS for a split of each sample solution; external precisions on  $^{147}\text{Sm}/^{144}\text{Nd}$  and  $^{176}\text{Lu}/^{177}\text{Hf}$  are  $\pm 2\%$ , and duplicate analyses on a small dataset by isotope dilution methods suggest accuracy better than 2% for Sm-Nd and 3% for Lu-Hf. Monte Carlo simulations suggest that these uncertainties are a very minor component of the overall uncertainty budget in age corrected epsilon values which are dominated by the measurement uncertainty on the isotope ratio. In cases where reliable whole rock samples were unavailable (e.g Tanzania), perovskite data have been used. These were obtained by similar procedures to those documented above.

Data for the western Canada kimberlites were obtained at both the NERC Isotope Geosciences Laboratory (NIGL), Keyworth, U.K. and Durham University, U.K. Full details of the dissolution and sequential extraction of Hf and Nd can be found in Dowall et al.<sup>39</sup>. In brief, 100mg of agate-milled powder was dissolved in concentrated HF-HNO<sub>3</sub> at 120°C for 3 days followed by repeat dry-downs in concentrated HNO<sub>3</sub> and then 6M HCl to break down fluorides.

Following dissolution, a cation exchange resin column was used to collect Hf and REE fractions. Nd was analysed on the REE fraction without further processing to remove Sm (see below). The Hf fraction was processed through a second anion exchange column to remove Ti before analysis. The majority of samples were analyzed for both Hf and Nd isotopic composition on a Neptune multi-collector ICP-MS at Durham University although a small subset of samples (identified in the Source data Table) were analyzed for Nd on a MAT-262 TIMS and for Hf on a P54 multi-collector ICP-MS at NIGL. Those samples analysed for Nd

isotopes by TIMS at NIGL were further processed through HDEHP columns to obtain a Sm-free pure Nd fraction.

For Nd analysis by MAT-262 TIMS, instrumental mass bias was corrected using a  $^{146}\text{Nd}/^{144}\text{Nd}$  ratio of 0.7219 and an exponential law while, for Nd analysed on the Neptune, mass bias was corrected using a  $^{146}\text{Nd}/^{145}\text{Nd}$  ratio of 2.079143 (equivalent to a  $^{146}\text{Nd}/^{144}\text{Nd}$  ratio of 0.7219). The  $^{146}\text{Nd}/^{145}\text{Nd}$  ratio was employed as Nd was measured on a total REE-cut from the first cation column stage, and this is the only Ce and Sm-free stable Nd isotope ratio. This approach obviously requires a correction for isobaric interferences from Sm on  $^{144}\text{Nd}$ ,  $^{148}\text{Nd}$  and  $^{150}\text{Nd}$  and is described in ref.40. The accuracy of the Sm correction method during analysis of a total REE fraction is demonstrated by repeat analyses of BHVO-1, which provided an average  $^{143}\text{Nd}/^{144}\text{Nd}$  ratio of  $0.512982 \pm 0.000007$  (13.5 ppm 2SD; n=13) after the Sm correction; identical to the TIMS ratio of  $0.512986 \pm 0.000009$  (17.5 ppm 2SD; n=19) based on purified Nd cuts<sup>41</sup>.

For Hf isotope analysis on the P54 and Neptune, instrumental mass bias was corrected using a  $^{179}\text{Hf}/^{177}\text{Hf}$  ratio of 0.7325. The Hf isotope composition of BHVO-1 analysed on the same dissolutions on which Nd data were obtained yielded an average  $^{176}\text{Hf}/^{177}\text{Hf}$  of  $0.283104 \pm 0.000008$  (28.3 ppm 2SD; n=13), identical to reference values<sup>41</sup>. All western Canada kimberlite  $^{143}\text{Nd}/^{144}\text{Nd}$  and  $^{176}\text{Hf}/^{177}\text{Hf}$  ratios are reported relative to La Jolla Nd = 0.511860 and JMC475 = 0.282160, respectively. External precisions (2SD) for data obtained at Durham are better than  $\pm 0.000018$  (including analysis of pure and Sm-doped J&M isotope reference material) and  $\pm 0.000012$  respectively, and for data obtained at NIGL are  $\pm 0.000019$  and  $\pm 0.000012$  respectively, based on repeat analysis of isotope reference materials J&M and JMC 475 during each analytical session.

$\epsilon\text{Nd}$  and  $\epsilon\text{Hf}$  values were calculated using the chondrite compositions of Bouvier et al<sup>15</sup>. The half-lives of  $^{147}\text{Sm}$  and  $^{176}\text{Lu}$  used are  $6.54\text{E}^{-12}/\text{yr}$  and  $1.867\text{E}^{-11}/\text{yr}$ , respectively.

**Geochronology** For the majority of samples, literature age determinations have been used, and these are noted in the Supplementary Data table. For the Silvery Home kimberlite, a phlogopite Rb-Sr age was determined. Phlogopite samples were washed in hot water, spiked with an  $^{85}\text{Rb}$ - $^{84}\text{Sr}$  tracer and dissolved on a hotplate. Sr was extracted and purified using two passes over small (0.15 ml) beds of Eichrom<sup>TM</sup> Sr resin (50-100 mm), which reduced Rb and BaAr++ interference during Sr isotope analyses on the MC-ICPMS to negligible levels. Rb was purified using cation exchange and analysed using Zr-doping. Data for a single, unleached phlogopite fraction from Silvery Home yields a relatively low Rb/Sr and  $^{87}\text{Sr}/^{86}\text{Sr}$ . Combined with data for perovskite<sup>42</sup>, the phlogopite provides a 2-point Rb-Sr age of  $181.3\pm 1.6$  Ma consistent with, but more precise than, the LA-ICP-MS U-Pb age for perovskite of  $183\pm 35$  Ma<sup>43</sup>. See Extended data Table 1.

**Modelling alternative scenarios for generating the primitive kimberlite array** Two processes were explored as a means of generating the primitive kimberlite data arrays through time (Fig. 1) and deviations from CHUR (Fig. 2). See Extended Data Table 2 for modelling parameters.

In the first we used the best-fit lines (albeit through somewhat scattered data), anchored to CHUR at 4.55 Ga in Figure 1 to provide an estimate of the present-day Nd and Hf isotope compositions of the PM source, and thus the parent-daughter ratios required for its evolution. Because the latter differ slightly from CHUR, isotopic compositions will necessarily depart from CHUR with time; a trajectory included in Fig 2 illustrates this effect that is, the isotopic variation that can be expected in this reservoir from radiogenic ingrowth alone. We note that, although the scatter in the measured data do not preserve a strict age progression (not shown), radiogenic evolution of this modelled source alone would generate

4-5 epsilon units of scatter (i.e., half of that observed) without recourse to any open-system processes (e.g., mixing).

In the second model, we simulated the incorporation of subducted slabs into a CHUR-like lower mantle source region, from which kimberlite melts were then produced. We ran numerous models allowing the N-MORB component to age by between 0 and 2 Ga prior to mixing of between 0 and 15% slab component into the PM source. Although the scatter in the data can accommodate the addition of between 0-10% slab of 0.5-1Ga at the time of mixing, the model arrays most closely approximating the data in Fig. 1 were generated via the continuous addition of 5% slab component (predominantly basalt although minor sedimentary components have little effect at such low slab involvement) that was 500 Ma old at the time of mixing into 95% CHUR, followed by the generation of kimberlite magmas (Extended Data Figure 1). Note that, although arithmetically achievable, even this mixing model requires a deep mantle reservoir with primordial compositional characteristics to provide most of the material input.

**Modelling the origins for the anomalous kimberlite arrays** The anomalous post 200 Ma kimberlite source is marked by a sudden departure from the main primitive kimberlite evolutionary trend followed by a relatively rapid track back towards this array (Fig. 3).

Although crustal contamination has the potential to shift Nd and Hf isotope ratios to lower values, it is hard to envisage any scenario in which such processes would be suddenly initiated in three widely dispersed continental locations at circa 200 and 100 Ma (Fig 3). Furthermore, the linear arrays evolving with time back towards the mantle array would require a highly systematic control – whereas crustal contamination is usually seen as a more random process, and zircon megacrysts, which have not experienced any upper level crustal

contamination, show very similar time-composition relationships<sup>44</sup>. Finally, any kimberlite experiencing such extreme levels of crustal contamination would no longer retain its primary magmatic characteristics. For all these reasons, and the fact that samples have been filtered for crustal contamination effects, we consider crustal contamination an unlikely scenario for generating these arrays.

The geographic arrangement of these sites (Extended Data Figure 2) suggests a possible link with palaeo-subduction events and it is accepted that subducted slab signatures can produce the general form of the Nd-Hf mantle array<sup>21</sup>. A number of these anomalous kimberlites from southern Africa, Brazil and western Canada also exhibit elevated Sr-isotope ratios with  $^{87}\text{Sr}/^{86}\text{Sr}$  up to 0.706 further suggestive of a subduction influence<sup>42,45</sup>. We have proposed in the main text that subducted slabs, ponding at the transition zone and eventually (around 200 Ma) avalanching into the lower mantle, may have triggered these remarkable departures from the primitive kimberlite evolutionary trend by the incorporation of ancient subduction components. Here we further explore two aspects of this hypothesis: first, the processes required to attain these unusual isotopic shifts, and secondly the nature of the steep linear arrays observed in time vs compositional space.

**The origin of the enriched isotopic signatures** The unusual departures from the mantle array witnessed in the post-200 Ma kimberlites from southern Africa, western Canada and Brazil require ancient sources with a protracted history of evolution under sub-chondritic parent/daughter ratios. Following the approach of Chauvel et al.<sup>21</sup> we modelled the likely effect of subducting ancient slabs (basalt plus sediment) into the deep mantle and storing them there to be tapped by post-200 Ma kimberlite magmatism.

Employing a conservative mixture of 90% MORB:10% sediment in the subducting slab assemblage, we find that the first expression of both the southern African and western

Canada anomalous kimberlites (i.e. those with the most significant departure from the mantle array) could be generated from ancient slabs subducted into the mantle (Fig 3) but that these would have to be of the order of 3-3.5 Ga in age to accommodate the large isotopic shifts observed – at least with the parameters used in our study. These represent minimum values as our calculation does not consider the effects of subsequent mantle mixing which will shift compositions to more radiogenic values. We find that terrestrial sediments provide a better fit than pelagic sediments in such a model: pelagic sediments can be used but require a larger proportion of sediment, or an older slab. The Brazil array is insufficiently well-characterised at present to enable a similar calculation. Ultimately metasomatic processes, linked to subduction, may provide a more tractable solution to this problem but investigation of such phenomena is beyond the scope of this study.

**The origin of the linear arrays with time** The steep linear trends observed with time in these three kimberlite suites suggest a very well-defined chemical evolution. Perhaps the most obvious way of achieving this would be to mix the slab component with a depleted asthenospheric mantle upon eruption: in Extended Data Figure 3 we explore this possibility. For simplicity, we ignore prior mixing with PM in this calculation and focus entirely on mixing slab components with depleted upper mantle on kimberlite ascent. It is important to note that kimberlite melts of any given age must mix with DMM of the *same* age and, as a result, all mixing vectors are vertical in this diagram. As such any constant proportion of DMM entrainment will not produce the steep arrays noted in anomalous kimberlite data. The only way to generate such arrays would be by the progressive and substantial increase in the DMM component with successive magmatic episodes (vertical displacement) somehow also highly correlated with the age of mixing (horizontal displacement). Such a process seems unlikely as the trace element compositions of the kimberlites do not change through time and

the same process would have to be mirrored on three different continents. Similar vectors are obtained by mixing with primitive rather than depleted mantle.

Since mixing does not appear to be able to generate the steep trends observed in the kimberlite data a second possibility is that radiogenic ingrowth within the source itself could account for the sub-parallel trends observed – indeed we invoked a similar model for the genesis of steep time-composition relationships observed in the zircon megacrysts<sup>44</sup> which are found in some kimberlites. It is important to note, however, that such radiogenic ingrowth would require highly elevated parent/daughter ratios in the source (in the case of the southern Africa dataset these are  $^{176}\text{Lu}/^{177}\text{Hf}$  of 0.326 and  $^{147}\text{Sm}/^{144}\text{Nd}$  of 0.78, and in the case of western Canada even more extreme values of 0.963 and 1.07 for  $^{176}\text{Lu}/^{177}\text{Hf}$  and  $^{147}\text{Sm}/^{144}\text{Nd}$  respectively). Such ratios could only be attained under the influence of garnet and would therefore impose strong constraints on the maximum depth of the source rocks, and perhaps involve carbonatite metasomatism to produce highly elevated parent/daughter ratios at the outset<sup>43</sup>.

### **References for online Methods section and Extended Data**

30. Clement, C.R. A comparative geological study of some major kimberlite pipes in Northern Cape and Orange Free State. Unpublished PhD thesis, University of Cape Town 728pp (1982).
31. Kjarsgaard, B.A., Pearson, D.G., Tappe, S., Nowell, G.M. & Dowall, D.P. Geochemistry of hypabyssal kimberlites from Lac de Gras, Canada: comparisons to a global database and applications to the parent magma problem. *Lithos* **112S**, 236-248 (2009).
32. Le Roex, A.P., Bell, D.R. & Davis, P. Petrogenesis of Group I kimberlites from Kimberley, South Africa: evidence from bulk rock geochemistry. *J. Petrology* **44**, 2261-2286 (2003).

33. Heaman, L.M. & Kjarsgaard, B.A. Timing of eastern North American kimberlite magmatism: continental extension of the Great Meteor hotspot track? *Earth Planet Sci. Lett.* **178**, 253-268 (2000).
34. Eggins S. M. et al. A simple method for the precise determination of  $\geq 40$  trace elements in geological samples by ICPMS using enriched isotope internal standardisation. *Chem. Geol.* **134**, 311–326 (1997).
35. Ottley, C. J., Pearson, D. G. & Irvine, G. J. A routine method for the dissolution of geological samples for the analysis of REE and trace elements via ICP-MS. In: *Plasma source mass spectrometry – applications and emerging technologies* (eds. G. Holland and S. D. Tanner). Royal Society of Chemistry, Cambridge. 221-230 (2003).
36. Münker, C, Weyer, S, Scherer, E & Mezger, K. Separation of high field strength elements (Nb, Ta, Zr, Hf) and Lu from rock samples for MC-ICPMS measurements. *Geochemistry, Geophysics, Geosystems*, **2**, 10.1029/2001GC000183 (2001).
37. Pin, C & Santos-Zalduegui, J.F. Sequential separation of light rare-earth elements, thorium and uranium by miniaturized extraction chromatography: application to isotopic analyses of silicate rocks. *Analytica Chimica Acta* **339**, 79-89 (1997).
38. Jweda, J, Bolge, L, Class, C & Goldstein, S.L. High precision Sr-Nd-Hf-Pb isotopic compositions of USGS reference material BCR-2. *Geostandards and Geoanalytical Research* **40**, 101-115 (2016).
39. Dowall, D. P., Nowell, G. M. & Pearson, D. G. Chemical pre-concentration procedures for high-precision analysis of Hf-Nd-Sr isotopes in geological materials by plasma ionisation multi-collector mass spectrometry (PIMMS) techniques. In: *Plasma source mass spectrometry – applications and emerging technologies* (eds. G. Holland and S. D. Tanner). Royal Society of Chemistry, Cambridge. 321-337 (2003).

40. Nowell, G. M. & Parrish, R. R. Simultaneous acquisition of isotope compositions and parent/daughter ratios by non-isotope dilution solution-mode plasma ionisation multi-collector mass spectrometry (PIMMS). In: *Plasma source mass spectrometry: the new millennium* (eds. J. G. Holland and S. D. Tanner). Royal Society of Chemistry, Cambridge. 298-310 (2001).
41. Weis, D., Kieffer, B., Maerschalk, C., Pretorius, W. & Barling, J. High-precision Pb-Sr-Nd-Hf isotopic characterization of USGS BHVO-1 and BHVO-2 reference materials. *Geochemistry, Geophysics, Geosystems* **6**, Q02002 (2005).
42. Woodhead, J., Hergt, J., Phillips, D. & Paton, C. African kimberlites revisited: in situ Sr-isotope analysis of groundmass perovskite. *Lithos* **112**, 311–317 (2009).
43. Griffin, W.L. et al. Emplacement ages and sources of kimberlites and related rocks in southern Africa: U-Pb ages and Sr-Nd isotopes of groundmass perovskite. *Contributions to Mineralogy and Petrology* **167**, 1032 (2014).
44. Woodhead, J., Hergt, J., Giuliani, A., Phillips, D., Maas, R. Tracking continental-scale modification of the Earth's mantle using zircon megacrysts. *Geochemical Perspectives Letters*. 4,1727 (2017).
45. Tappe, S., Pearson, D.G., Kjarsgaard, B.A., Nowell, G., Dowall, D. Mantle transition zone input to kimberlite magmatism near a subduction zone: origin of anomalous Nd-Hf systematics at Western Canada, Canada. *Earth Planet Sci. Lett.* **371-372**, 235-251 (2013).
46. Odin, D.S. and 35 collaborators (1982), Interlaboratory standards for dating purposes, Odin, G.S. (editor) Numerical Dating in Stratigraphy. Part 1. John Wiley & Sons, Chichester, 123-148.
47. Gale, A., Dalton, C.A., Langmuir, C.H., Su, Y., Schilling, J.-G. The mean composition of ocean ridge basalts. *Geochem. Geophys. Geosyst.* **14** (3), 489–518 (2013).

- 48 Vervoort, J.D., Blichert-Toft, J. Evolution of the depleted mantle: Hf isotope evidence from juvenile rocks through time. *Geochimica et Cosmochimica Acta* **63**, 533-556. (1999)
- 49 Chauvel, C. et al. Constraints from loess on the Hf-Nd isotopic composition of the upper continental crust. *Earth Planet. Sci. Lett.* **388**, 48-58 (2014).
50. Scherer, E., Munker, C., Mezger, K. Calibration of the lutetium-hafnium clock, *Science* **293** 683-687(2001).
51. Söderlund, U., Patchett, P.J., Vervoort, J.D., Isachsen, C.E. The  $^{176}\text{Lu}$  decay constant determined by Lu-Hf and U-Pb isotope systematics of Precambrian mafic intrusions. *Earth Planet. Sci. Lett.* **219**, 311-324.
52. Lugmair, G.W., Marti, K. Lunar initial  $^{143}\text{Nd}/^{144}\text{Nd}$ : differential evolution of the lunar crust and mantle. *Earth Planet. Sci. Lett.* **39**, 349-357 (1978).
53. Scotese, C.R. PALEOMAP PaleoAtlas for GPlates and the PaleoData Plotter Program, PALEOMAP Project, <http://www.earthbyte.org/paleomap-paleoatlas-for-gplates/> (2016)
54. Müller, R.D. et al. Ocean basin evolution and global-scale plate reorganization events since Pangea breakup. *Annual Rev. Earth. Planet. Sci.* **44**, 107-138 (2016).

## Extended Data legends

### Extended Data Table 1 | Isotope data used to generate an age for the Silvery Home

**kimberlite.** \*Model ages for GLO-1 calculated with initial  $^{87}\text{Sr}/^{86}\text{Sr} = 0.7074$

Mass bias in Sr isotope runs corrected by internal normalization to  $^{88}\text{Sr}/^{86}\text{Sr} = 8.37521$  using the exponential law,  $^{87}\text{Sr}/^{86}\text{Sr}$  is reported relative to SRM 987 = 0.710230 and has an external precision of  $\pm 0.000040$  (2sd), mass bias in spiked Rb runs corrected by normalization to

$^{90}\text{Zr}/^{91}\text{Zr} = 4.584514$  in dopant Zr,  $^{87}\text{Rb}/^{86}\text{Sr}$  obtained by isotope dilution has an external precision of  $\pm 0.5\%$  (2sd).

### **Extended Data Table 2 | Modelling parameters used in this study**

#### **Extended Data Figure 1| A model for generating the primitive kimberlite array**

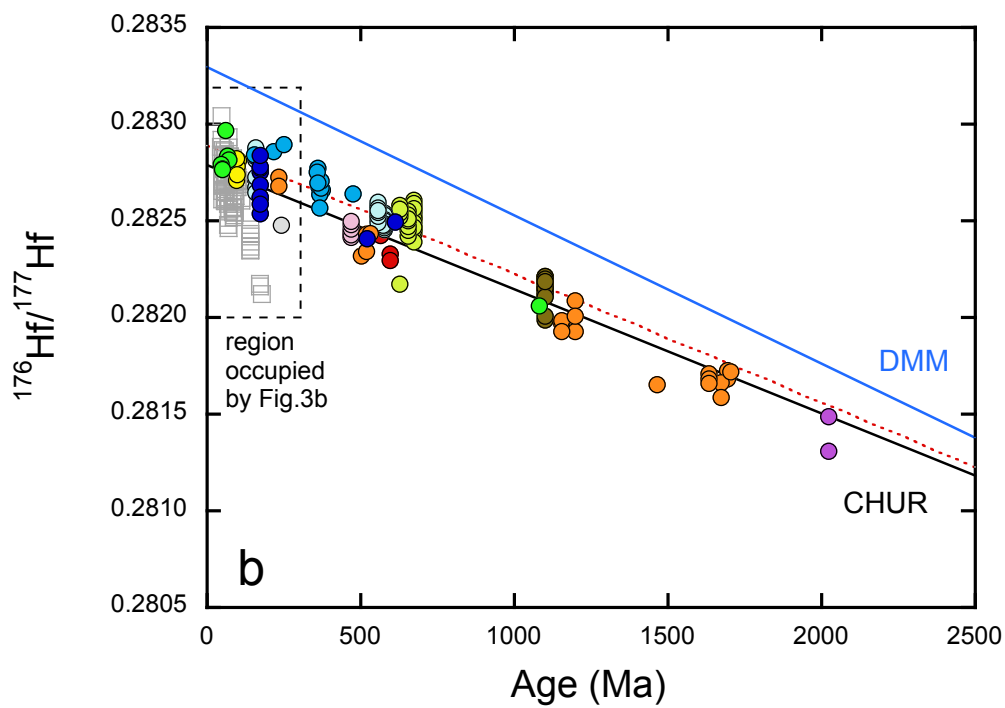
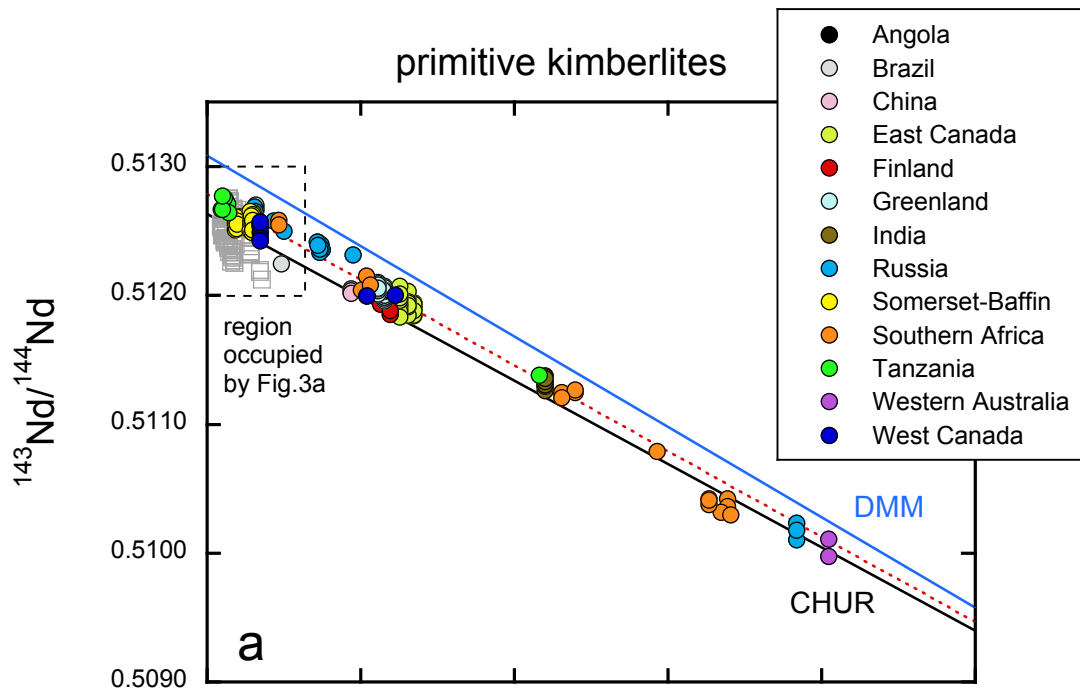
Model simulating the (a) Nd and (b) Hf isotope variations generated by the incorporation of subducted slab (N-MORB plus 0- 5% sediment) into a CHUR-like lower mantle source region from which kimberlite melts are produced. The best-fit to the observed data is achieved via the continuous addition (black arrows) of a 5% slab component (N-MORB in this illustration) that has been allowed to age by 500 Ma (green arrows) prior to mixing with the CHUR source (95%; panel c). Evolution trajectories similar to the green arrows for N-MORB are generated in the model when incorporating a sedimentary component (not shown here for clarity). Note that the addition of 95% of a deep mantle reservoir with PM compositional characteristics would still be required as a starting point for each mixing step.

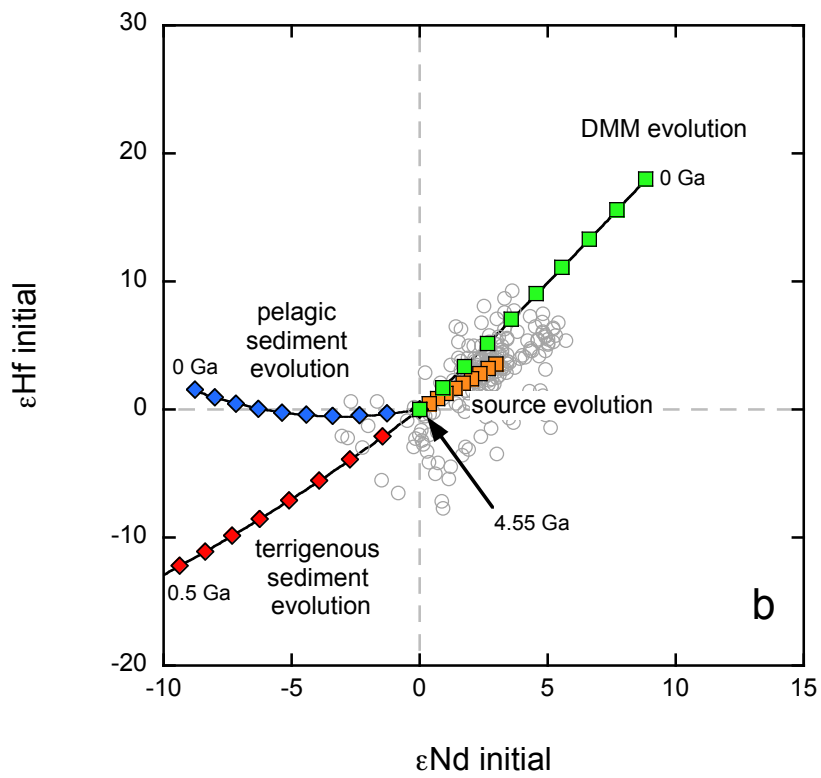
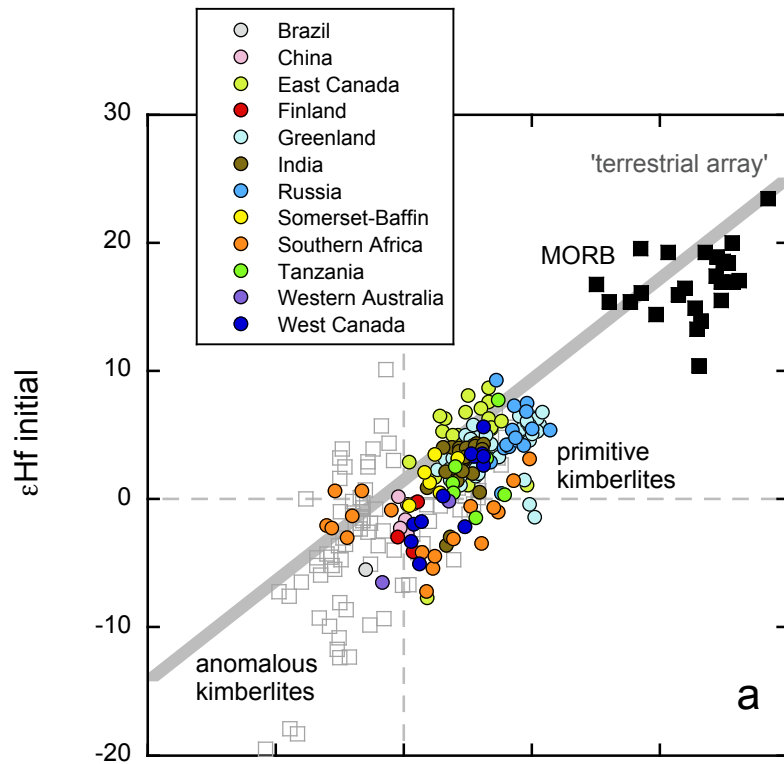
#### **Extended Data Figure 2| Reconstructions of the Pangea supercontinent at 200 Ma.**

Figure produced using PALEOMAP<sup>53</sup> and GPlates 2.0. White circles provide indicative locations for ‘primitive’ kimberlites, and gold circles indicate ‘anomalous’ kimberlite localities. Red lines indicate subduction zones at the western edge of Pangea<sup>54</sup>.

**Extended Data Figure 3| Subducted slab-DMM mixing arrays in relation to the anomalous kimberlite data.** Although assimilation of DMM by an ascending enriched ‘kimberlite’ component might be considered the most obvious way of generating the steep data arrays in the anomalous kimberlites, melts of any given age must mix with DMM of the

*same* age. Thus, mixing vectors do not point towards modern DMM, they are vertical in age vs isotope ratio diagrams. Consequently, any constant proportion of DMM entrainment will not produce the steep arrays noted in the anomalous kimberlite data. Instead, a progressive and substantial increase in the DMM component with successive magmatic episodes (vertical displacement) would be required, somehow also highly correlated with the age of mixing (horizontal displacement). Similar vectors are obtained by mixing with Primitive rather than Depleted mantle.





anomalous kimberlites

